Uluslararası İleri Doğa Bilimleri ve Mühendislik Araştırmaları Dergisi
Sayı 9, S. 90-101, 7, 2025

Araştırma Makalesi

IJANSER
https://as-proceeding.com/index.php/ijanser
ISSN:2980-0811

International Journal of Advanced Natural Sciences and Engineering Researches
Volume 9, pp. 90-101, 7, 2025

Research Article

Synthesis and characterization of carbon quantum dots with different methods using biomass and food sources: Determination of surface properties and particle diameters

Veli ŞİMŞEK[1*]

[1]*Chemical Engineering Department, Bilecik Seyh Edebali University, 11210, Gulumbe Campus, Bilecik/Turkey, veli.simsek@bilecik.edu.tr*

(Received: 01 July 2025, Accepted: 11 July 2025)

(4th International Conference on Trends in Advanced Research ICTAR 2025, July 04-05, 2025)

ATIF/REFERENCE: Şimşek, V. (2025). Synthesis and characterization of carbon quantum dots with different methods using biomass and food sources: Determination of surface properties and particle diameters, *International Journal of Advanced Natural Sciences and Engineering Researches*, 9(7), 90-101.

Abstract- Nowadays, carbon quantum dots (CQD), a member of the nanoparticle family, are gaining popularity due to their advantageous optical and energy properties. It is vital for the continued sustainability of the environment that the chemicals and processes used in the synthesis of such materials are eco- friendly. The aim of the research will be to synthesize biocompatible CQDs from various waste biomass sources that are carbon sources using green chemistry hydrothermal and solvent thermal methods, as well as to develop and modify surface properties. First, CQDs were synthesized from various biocompatible biomass sources using green chemical hydrothermal and solvothermal methods. The UV-VIS, FT-IR, SEM/EDX, MAPPING, ZETA sizer and fluorescent microscope analysis methods were used to examine the structural properties of the obtained CQDs. In addition, the color spectra of the dispersion samples were determined using a UV-Lamp. According to the obtained UV-VIS analysis results, it was determined that CQDs absorb light at 284nm. Although CQDs are transparent and yellow under daylight, they have been observed to emit a particularly bright blue fluorescence under UV light (365nm). Blue fluorescence spectrums in the literature indicate the presence of CQDs between 2 and 5 nm.

Keywords-Biomass, Morus Nigra L., Silybum Marianum, Cqds, Green Chemistry, Hydrothermal And Solvothermal Method.

I. INTRODUCTION

Today, the use of green chemistry synthesis methods in the synthesis of nano-particles(NPs) in order to develop sustainable production systems and use resources efficiently is attracting attention day by day. The development of synthesized NP properties is one of the main goals of scientists. In addition, it is among the targets to increase the environmentally friendly NP catalysis effects by using non-toxic, environmentally friendly chemicals and materials. These approaches are aimed at reducing the negative environmental impact of synthesis by reducing waste, solvents used during synthesis, precursors, and derivatives [1]. Moreover, in addition to the intensification of research on the use and applications of renewable raw materials, it has been observed that the green chemistry synthesis method in the synthesis

of CQDs has positive advantages (such as eco-friendly, low toxicity, energy-cost, reusability, safe and sustainable) [2].

CQDs are among the nanomaterials. Besides being nano-sized crystals, they have semiconductor properties [3]. Quantum dots (QDs) are generally artificial compounds obtained from the II-VI and III-V group compounds of the periodic table (for example, CdSe, CdTe, CdS, and ZnSe), and their diameters vary between 2 and 15 nm [4]. A semiconductor QD consists of a semiconductor core and a shell that protects the core from oxidation and increases the quantum yield [5]. In applications, the performance of QDs can be increased with the help of the hydrophobic or hydrophilic nature of the shell surface and the ligands used. Semiconductor NPs have a wide range of applications such as biotechnology, electronics, laser systems, optical circuits, and marking due to their different optical and energy properties depending on different particle sizes. One of the features that makes semiconductors important is their electrical conductivity, which can be changed during use with some external stimuli (voltage and temperature difference, photon bombardment) after production. These properties have made it possible to use light-emitting diodes (LEDs) in the imaging industry. The use of CNs, which have an energy band gap to adapt to the wavelengths of the rays coming from the sun, in solar cell studies has added a new dimension to the studies and increased the studies of scientists on this subject. The use of CNs in biotechnological applications has increased in parallel with the rapid developments in nanotechnology, and an important step has been taken in bioimaging, diagnosis, and follow-up of diseases in the fields of medicine and biology [2].

Recently, the reasons for the use of biomass-derived and biocompatible CQDs instead of toxic QDs in the field of health include modification of their sizes depending on the synthesis methods, irradiation in different colors (spectra) thanks to their crystal sizes, and their use as fluorescent probes for medical diagnosis and imaging. They are biocompatible and use biomass as a carbon source in their production.

CQDs are obtained with dots top-down and bottom-up approaches [6], electrochemical carbonization [7, 8], laser ablation [9, 10], and microware irradiation [11-13] methods. However, hydrothermal/solvothermal methods are preferred because of their cheap costs, ease of application and environmental (non-toxic) properties [14-20].

Silybum marianum (Virgin Mary Thistle) is a source of biomass. Seeds of *Silybum marianum* contain 1 to 6% silymarin ($C_{25}H_{22}O_{10}$). Important compounds such as silybin, silydianin, and silicristin are found in silymarin, which is responsible for pharmacological action [21]. On the other hand, studies have shown that *Morus nigra* L (Black Mulberry BM) has important effects on human health and nutrition due to its phenolic compounds, organic acids and sugar content [22]. The main content of black mulberry anthocyanins on lung cancer cells reported to have an inhibitory effect cyanidin-3-glycoside($C_{21}H_{21}ClO_{11}$), cyanidin-3-rutinoside($C_{27}H_{31}ClO_{15}$), pelargonidin-3-glycoside ($C_{15}H_{11}ClO_5$) and pelargonidin-3- rutinosite($C_{27}H_{31}O_{14}^{+}$) [23-25].

In this study, which was carried out, the production of CQDs by green chemistry hydrothermal/solvothermal synthesis methods using different biomass waste and food sources such as *Silybum marianum* (Virgin Mary Thistle(VMT)), and *Morus nigra* L (Black Mulberry Jam BMJ; homemade) BMJ. Furthermore, the surface charges of the obtained CQDs were examined(CQDs obtained from VMT and BMJ were called as sample 1 and 2, respectively). It was observed that the applied synthesis method may be successful in obtaining CQDs of the desired sizes. One of the unique features of the method used in the synthesis of CQDs is that it is both environmentally friendly and biocompatible. Furthermore, the effects of synthesis temperature, raw material amount, solvent amount, and synthesis times on the sizes and yields of CQDs will be investigated in future studies.

This presented paper has been successfully realized on the obtained CQDs with UV-VISIBLE (for determining light absorption values) and FT-IR (for determining functional groups). Images of carbon quantum dot samples under UV light were performed using a UV fluorescent lamp with a wavelength of 365 nm. In addition, fluorescent microscope analyses on samples 1 and 2 were performed using 5 different filters at wavelengths (emissions) of 420-460, 600, 400-440, 575-625, and 510-550nm. The data obtained are given in detail in the results section.

II. MATERIALS AND METHODS

Synthesis of CQDs

A new recipe was created according to the results obtained after the literature review. First, CQDs were synthesized using green chemistry hydrothermal/solvothermal methods at different temperatures and times with certain biocompatible biomass sources. The schematic representation of the synthesis methods is given in Figure 1 in detail.

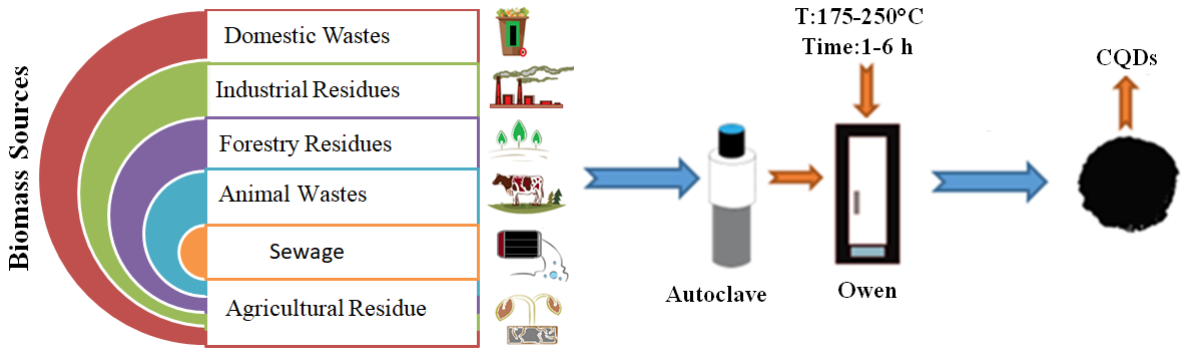

Fig. 1 Synthesis procedures of CQD.

Synthesis steps:

-First, the biomass and food resources were prepared (pre-treatment is done by grinding and crushing). Moreover, jam made from natural blackberries was used as a raw material (carbon quantum) source.

-It was sifted(especially biomass samples) after grinding (for a sample with a homogeneous diameter).

-Biomass samples of the determined amount and diameter were weighed separately and placed in a Teflon autoclave by adding a certain amount of solvent (pure water (H_2O) was used as a solvent for the hydrothermal method, and a water/ethanol (C_2H_5OH) mixture was used for the solvothermal method). Then it was kept in an oven at the specified temperature and time(Figure 1). The sample, which was removed from the oven, was dispersed in 20 ml of water by grinding with a mortar after cooling. After the dispersion process, 10 ml samples were taken and centrifuged at 4500 rpm for 2min.. Then, 2 mL samples were prepared by taking from the upper clear sample part. Afterward, samples were centrifuged at 15,000 rpm for 30 min.

III. RESULTS AND DISCUSSION

Characterization studies

Following centrifugation, the liquid and solid components were separated. The obtained samples were analyzed using UV-VIS instrument between 280 and 600 nm. The results are given in Figure 2 (a). The obtained results showed that the synthesized CQDs had spectrum values less than 300 nm (284 nm). Furthermore, they were found to be compatible when compared to the literature studies obtained.

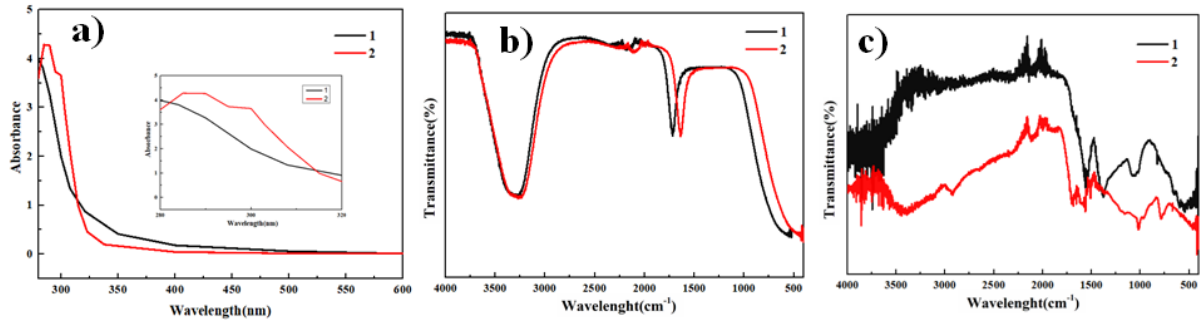

Fig. 2 a) Results of comparative UV-Vis analysis for samples 1 and 2, b) Results of comparative FT-IR analysis for samples 1 and 2(dispersion), c) Results of comparative FT-IR analysis for samples 1 and 2(solid phase).

FT-IR analyses of samples 1 and 2 were performed using the ATR (attenuated total reflection) method between 400 and 4000 cm^{-1} wavelengths. The biggest advantage of this technique is that it facilitates the analysis of liquid samples (Figure 2(a, b). Figure 2 (a) shows the FT-IR results for samples 1 and 2 in the liquid phase. It is predicted that the results being compatible with each other are due to the fact that the sizes of the CQDs in the liquid are in a certain range. It was observed that the FT-IR analysis results of the solid sample were consistent with the literature (Figure 2 (c)). Figure 2(b) shows the FT-IR results for samples 1 and 2 in the liquid phase. It is predicted that the results being compatible with each other are due to the fact that the sizes of the CQDs in the liquid are in a certain range. FTIR analysis of solid samples revealed the presence of several major bands. The one at 3310–3550 cm^{-1} (3345 cm^{-1}) in both spectra is usually attributed to OH stretching [26, 27] and H bonds in COOH groups, but it can also be attributed to alcohols, phenols, and even water. The weak stretching of the C-C bond can be seen in the broad absorption centered at 2265 cm^{-1} [26]. Furthermore, the three obvious absorption peaks at 2920 cm^{-1}, 1388 cm^{-1}, and 550-585 cm^{-1} are associated with the stretching and bending vibrations of CH, C=C, and =C-H, indicating the presence of alkyl and aryl groups, respectively [27]. The wide band gap of 3000-3500 cm^{-1} in the FTIR spectrum of the dispersion samples corresponds to the O-H and N-H structures [26, 27]. An aromatic C≡C structure was observed between wavelengths at 3200-3250 cm^{-1}. In the band gap of 2200–2100 cm^{-1} 1620-1640cm^{-1} [16], H-O-H, C=O, and C=C structures were obtained. In addition, the stretch between 1630-1720 wavelengths indicates the CH_3 structure [26].

Surface charges and particle size dispersion of synthesized carbon quantum dots by calculating the zeta potential were carried out. According to the results obtained, the zeta values were obtained as -6.5 mV and -2.92 mV, respectively. Zeta potential value stable importance for emulsion and suspension measurement carries. Above +25 mV of zeta potential or values below -25 mV the region where emulsions and suspensions are stable shows. If it is not between these values unstable and thus colloidal systems tend to agglomerate and precipitate [28]. Also, the surface charge values being close to zero may be very important for stability.

The particle size distribution of sample1 was observed to be concentrated between 15.64-24.36 nm and 255-712.4 nm (Figure 3 a, b). Sample 1 showed two different distributions, whereas sample 2 showed a single distribution(between 78,82-122,4 nm)(Figure 4 a, b). It is predicted that this situation is due to the fact that no tracking and ultrasonic treatment is applied on the samples before the analysis. That is, it is a result of agglomeration of the samples.

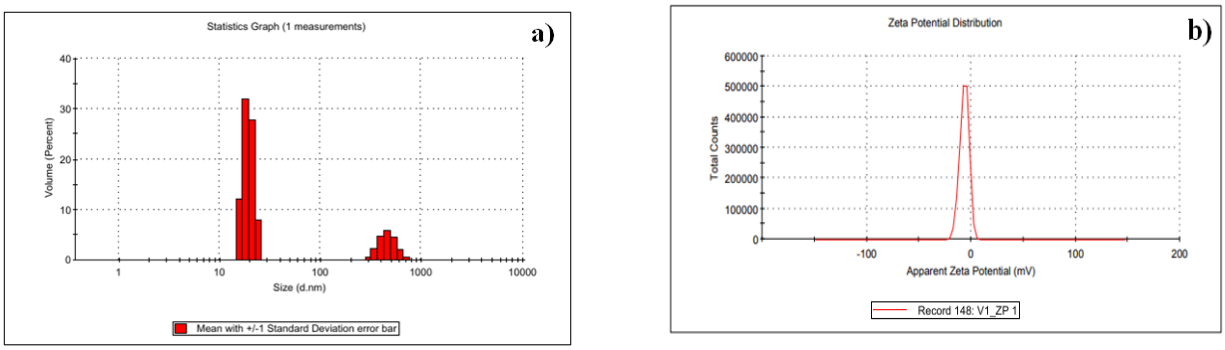

Fig. 3 The particle size distribution(a) and Zeta analysis (b) of sample1.

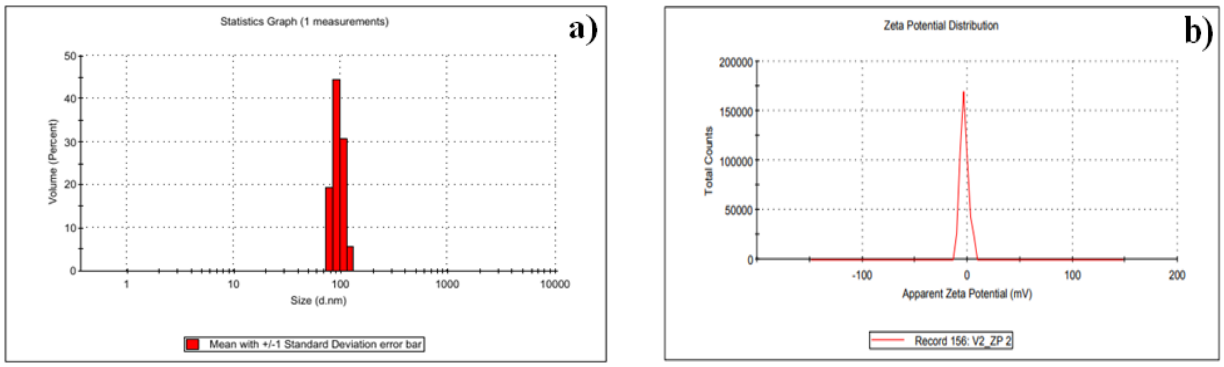

Fig. 4 The particle size distribution(a) and Zeta analysis (b) of sample2.

For SEM/EDX analyses, liquid samples (1 and 2) were dropped onto the sticky paper after filtration and centrifugation. Then, the drying processes were carried out under room conditions. Following that, SEM(Figure 5a-d), MAPPING (Figure 6a-d) and EDX(Table 1) analyses were performed. In particular, it was observed that the particles of sample 1 formed spherical structures by agglomeration (Figure 5 (a)). CQDs are a specific group of the previously described nanomaterials that are spherical objects of a size below 10 nm with a carbon core. According to the results obtained, it was predicted that the conditions used for centrifugation and filtration applied to CQDs should be improved. When the mapping analysis results are examined(Figure 6a-d), it is observed that the C element is very dense in the structure. In addition, these results are supported by EDX results(Table 1).

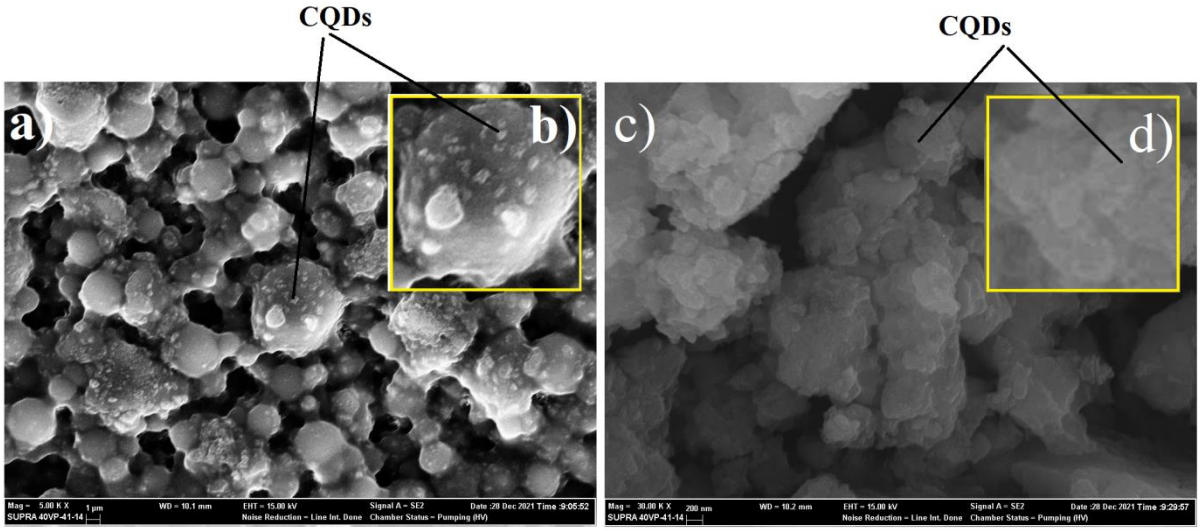

Fig. 5 SEM analyses of Sample 1 (a,b), and Sample2 (c,d).

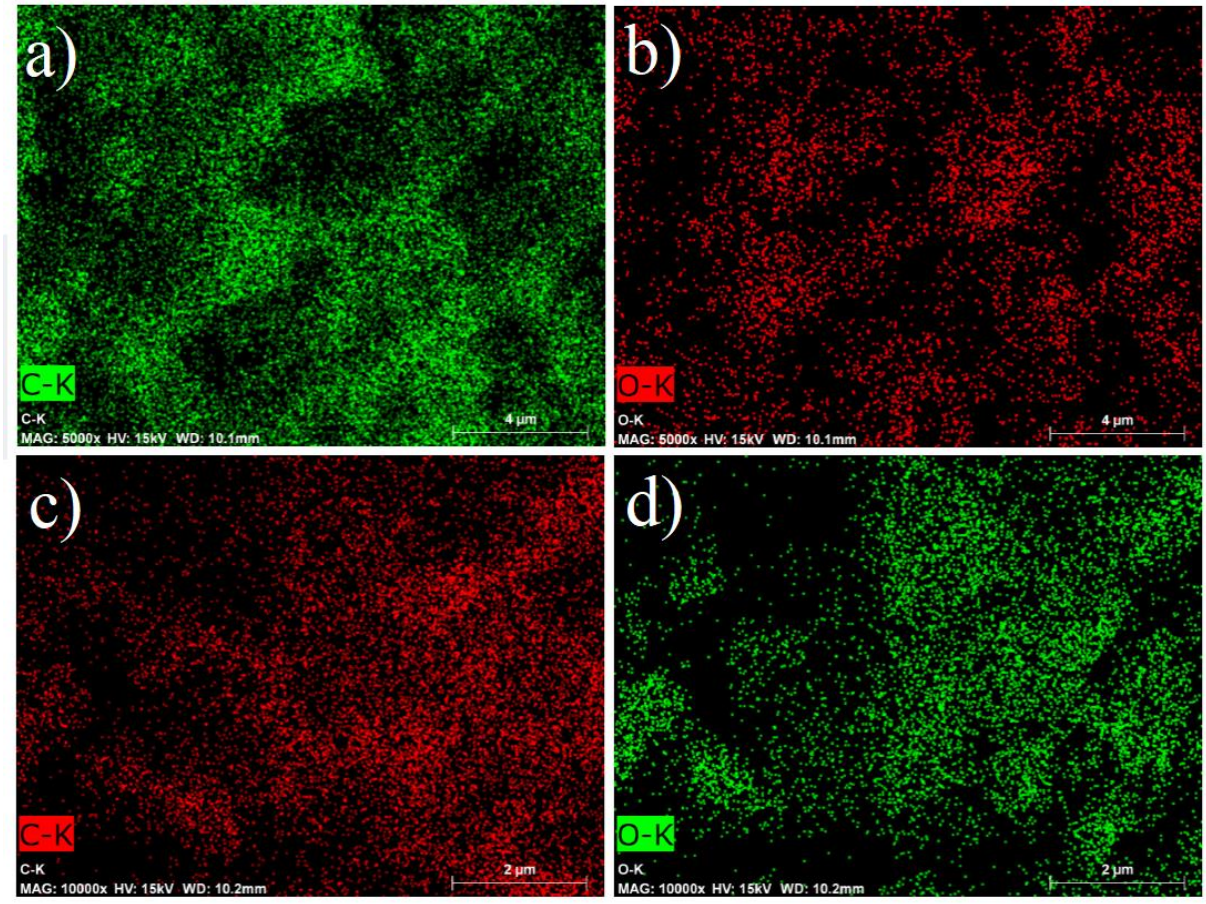

Fig. 6 MAPPING analyses of Sample 1 (a, b), and Sample2 (c,d).

In addition, fluorescent microscope analyses on samples 1 and 2 were performed using 5 different filters at wavelengths (emissions) of 420-460, 600, 400-440, 575-625, and 510-550 nm. The obtained results are given in Figures 7(a-e), and 8(a-e).

Table 1. EDX results of patterns.

CQDs	**C(% atom)**	**O(% atom)**
Sample 1	74.95	25.05
Sample 2	68.43	31.57

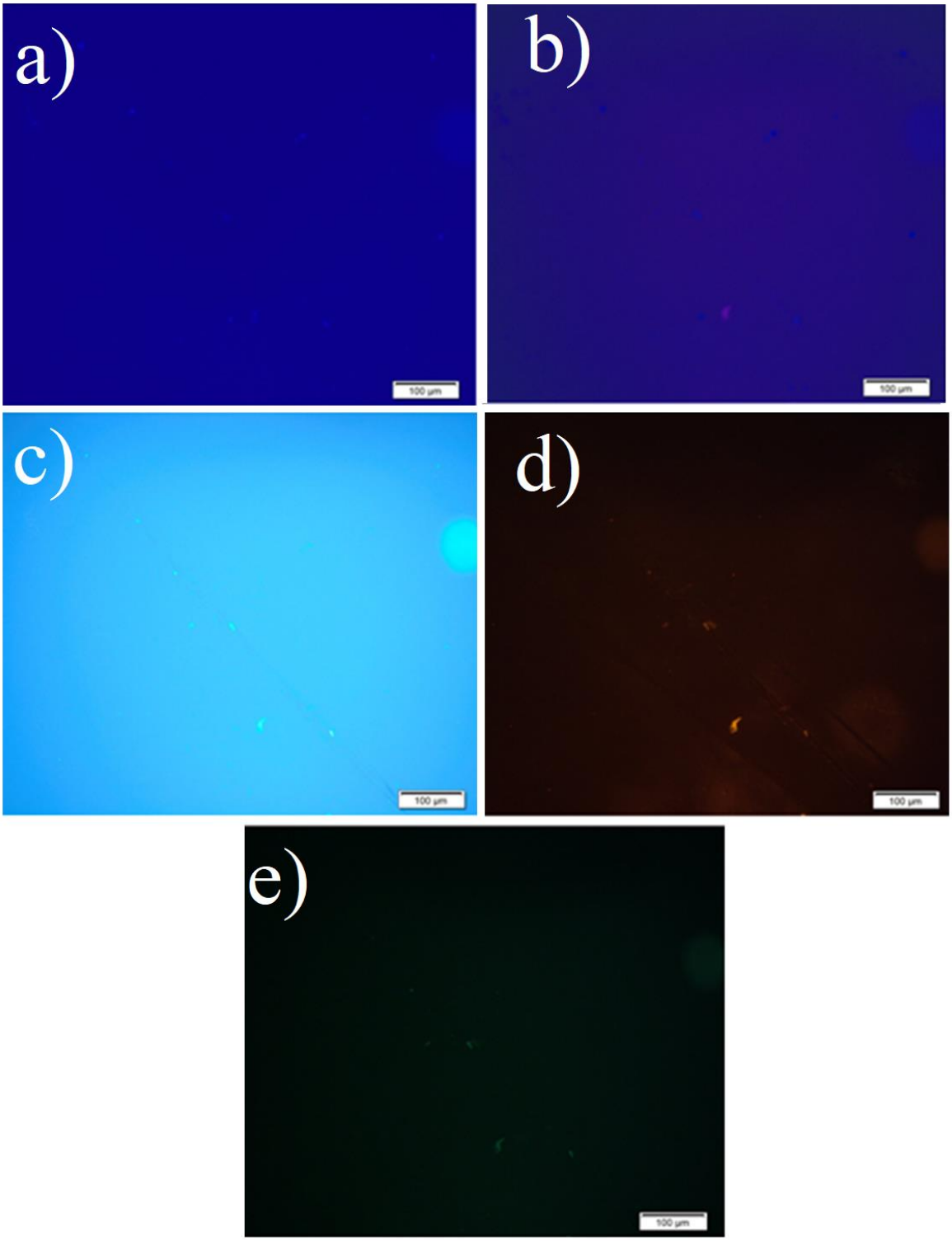

Fig. 7 Sample 1 Fluorescent microscope image a) 420-460nm, b) 600nm, c) 400-440nm, d) 575-625 and e) 510-550.

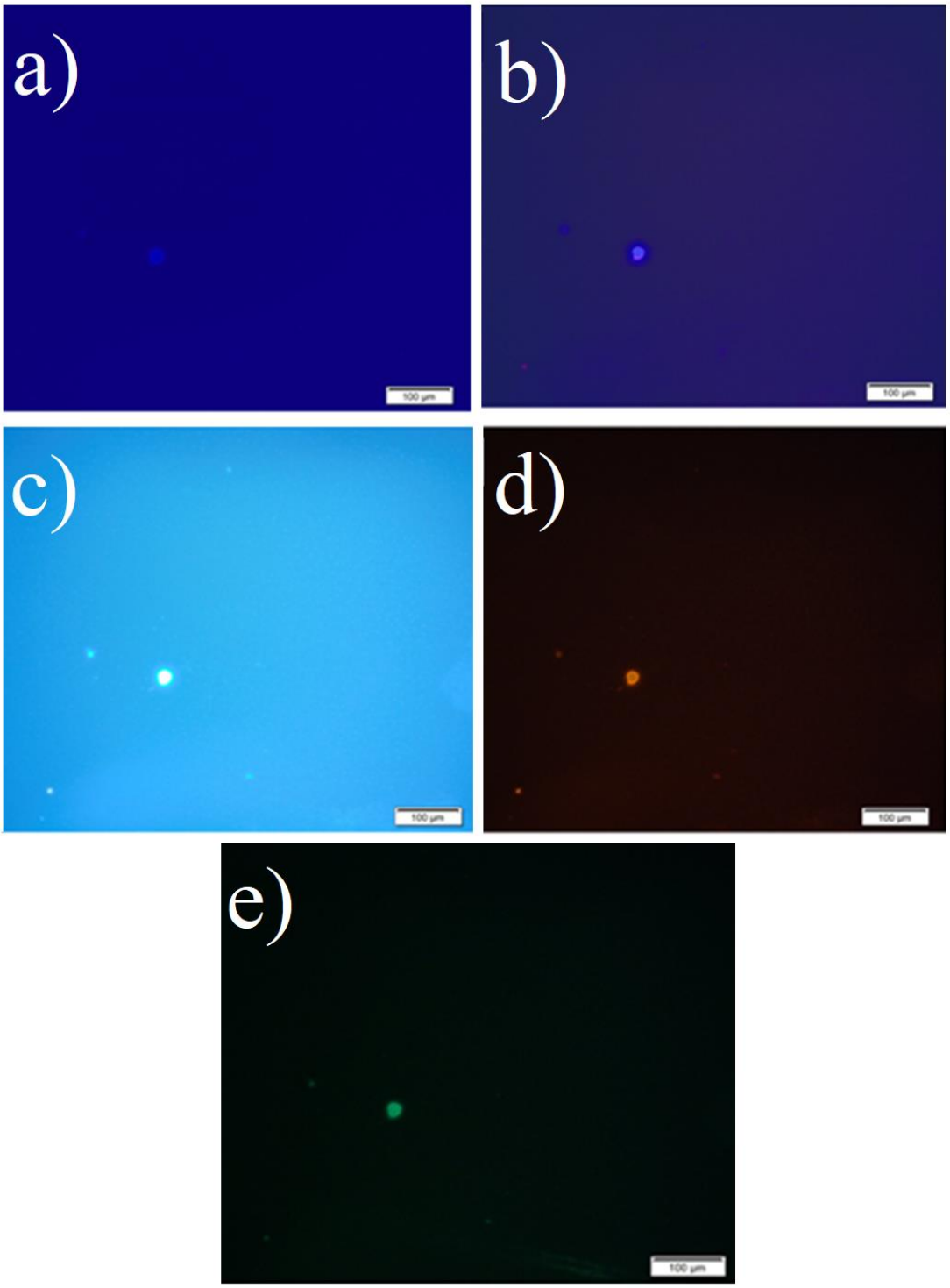

Fig. 8 Sample 2 Fluorescent microscope image a) 420-460nm, b) 600nm, c) 400-440nm, d) 575-625 and e) 510-550.

CQDs are not clearly visible on 100 µm scale images. However, when viewed in detail or when the images are enlarged, the CQDs appear to clump together (aggregate). It is known that in the visible region of the light and electromagnetic spectra, there is radiation of different colors depending on the material (atom or particle size) light interactions. It is seen that these radiations are observed in fluorescent microscope images (Picture 7, 8(a-e)). The color spectrums of CQDs samples under UV light were determined using a UV fluorescent lamp with a wavelength of 365 nm. The obtained images are shown in Figure 9(a-d). Although CQDs are transparent and yellow under daylight, they have been observed to emit a particularly bright blue fluorescence under UV light. Blue fluorescence spectrums correspond to the presence of CQDs between 2 and 5 nm.

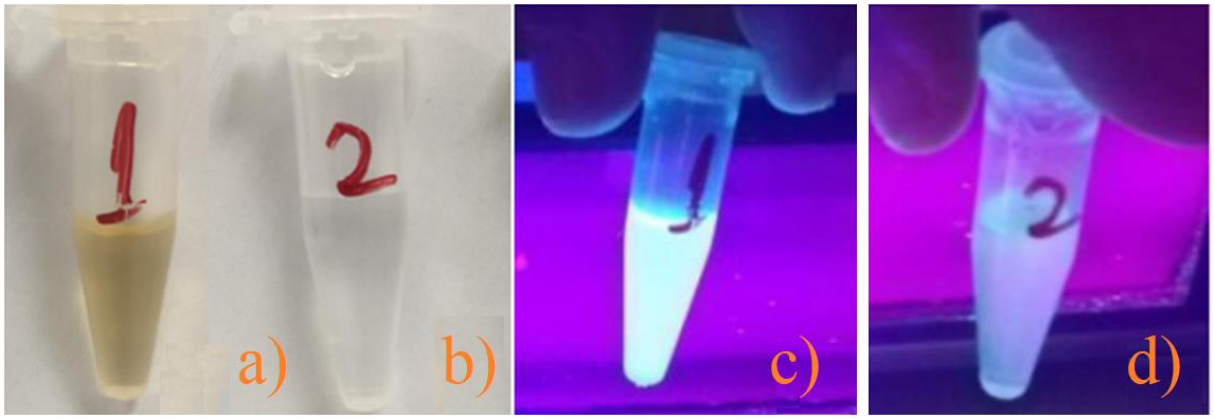

Fig. 9 365 nm UV-LAMB images of dispersion samples.

Additionally, fluorescent microscope images data and particle diameters of the samples with the Gaussian model were examined using the ImageJ (Fijiwin64-Fiji.app) program[29]. Figures 10 and 11 show estimated values obtained from fluorescent microscope images and the Gauss model, respectively. The zeta potential analysis, on the other hand, revealed that the particle sizes were around 100 nm (Figure 4 a). The reason the results are like this is that the CQDs are collected before analysis.

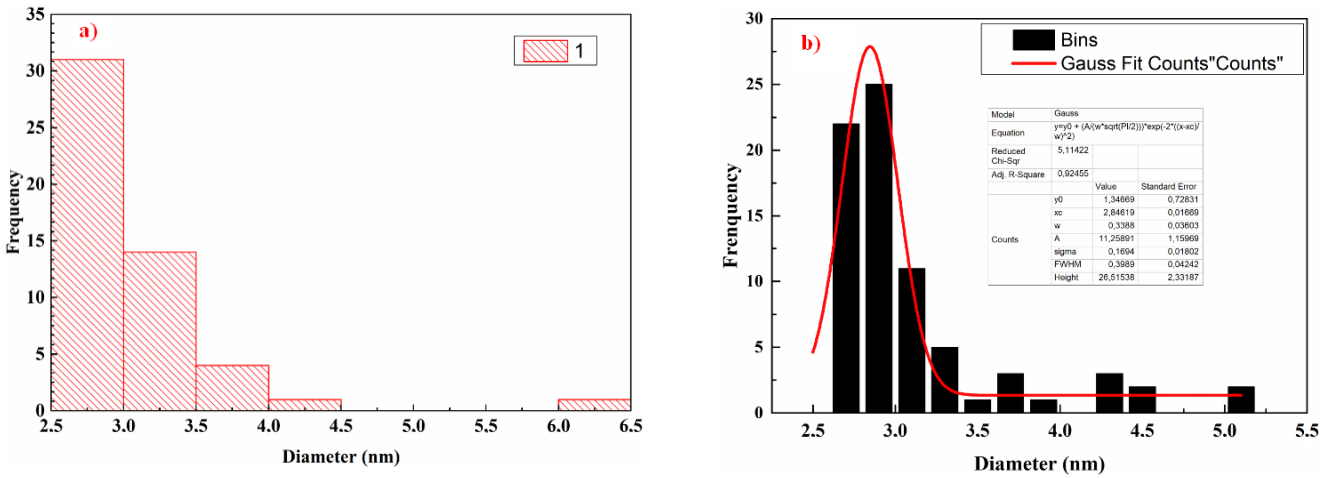

Fig. 10 The particle sizes dispersions (a) and R^2 (b) values of sample 1.

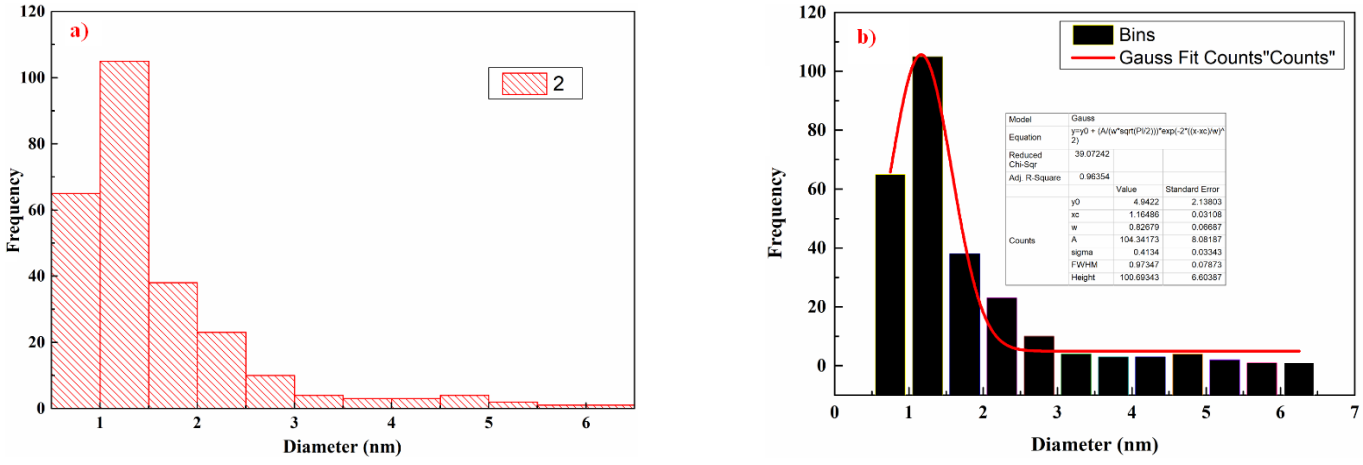

Fig. 11 The particle sizes, dispersions (a) and R^2 (b) values of sample 2.

When the fluorescent microscope images obtained at different emission values are examined, it can be thought that CQDs points of the desired sizes are not synthesized. CQDs are not clearly visible on 100 µm scale images. However, when viewed in detail or when the images are enlarged, the CQDs appear to clump together (aggregate). It is known that in the visible region of the light and electromagnetic spectra, there is radiation of different colors depending on the material (atom or particle size) light interactions. It is seen that these radiations are observed in fluorescent microscope images (Figure 7 and 8(a-e)). Especially the SEM images of sample 1 support this idea(Figure 5 a).

As a result of the characterization analysis performed, it was determined that the CQDs obtained were agglomerated rather than colloidal in structure. Accordingly, CQDs sizes were observed to be concentrated at 10 nm for Sample 1. However, it was determined that agglomeration was greater in Sample 2. On the other hand, it has been observed that they emit a particularly bright blue fluorescence under UV light. Moreover, the particle sizes, dispersions and R^2 values of sample 1 and 2 were calculated using the Gaussian method and images from a fluorescent microscope (emission wavelengths of 400–440 nm). R^2 values of sample 1 and 2 were obtained %92.425 and 96.354, respectively(Figures 10 and 11 (b)). According to the results obtained, the minimum, maximum, and average diameter values of CQDs were calculated as 2.61, 5.07, 3.078, 0.733, 6.18, and 1.537nm, respectively (Figure 10 and 11 (a , b).

The surface becomes negatively charged due to the ionization of surface groups and the dissociation of acidic groups on the surface. The surface becomes positively charged due to the dissociation of basic groups. The magnitude of the surface charge is determined by the acidic or basic strength of the surface groups as well as the pH of the solution. If all of the particles have a very large negative or positive zeta potential, they repel each other and the dispersion becomes stable. Dispersion instability (agglomeration and precipitation) occurs when the particles have a low zeta potential (between -30 and +30mV) because there is no force preventing the particles from aggregating (Figure 6). The negative charge formation on the surface of carbon quantum dots is due to NH_2 and OH groups [30].

IV. CONCLUSION

In this study, the synthesis of CQDs from biocompatible biomass and food sources using hydrothermal and solvothermal methods was investigated. The aim of the research was to synthesize novel types of biocompatible CQDs from various waste biomass and food sources that are carbon sources using green chemistry principles with hydrothermal and solvent thermal methods. In this context, it is anticipated that these preliminary studies will be useful for the evaluation of carbon quantum dots in different application areas(biological applications) in the future. Especially, the success of the functional groups of CQDs in bioapplications (such as imaging, biosensors, and drug delivery) depends on their interaction with structures such as NH_2. NH_2 group grafting with amines such as 2-ethylenediamine, poly(ethyleneamine), or trimethylamine can increase affinity to biological structures. Incorporation of nitrogen atoms improves resistance to photobleaching and imagining resolution. Also, nanodots are useful in the optical imaging of cancer cells and biomarkers.

According to the analysis results obtained, it is predicted that the surface functions and dimensions of CQDs will be modified. It was determined that the 15000 rpm centrifuge and the 0.22 µm filter used were not sufficient. However, it is thought that the desired sizes will be obtained by separating the aggregated CQDs from each other by sonic processing before the particle size analysis.

ACKNOWLEDGMENTS

I would like to thank Dr. Özge KAYGUSUZ İZGÖRDÜ for Fluorescent microscope analyses.

REFERENCES

[1] Rodríguez-Padrón D, Puente-Santiago AR, Balu AM, MuñozBatista MJ, Luque R: Environmental catalysis: present and future. ChemCatChem 2019, 11:18–38. https://doi.org/10.1002/ cctc.201801248.

[2] Sumiya Haque Adrita, Khandaker Nujhat Tasnim, Ji Hyun Ryu and Shazid Md. Sharker ,Nanotheranostic Carbon Dots as an Emerging Platform for Cancer Therapy, *J. Nanotheranostics* 2020, *1*(1), 58-77; DOI; https://doi.org/10.3390/jnt1010006.

[3] Zhua, C., Chen, Z., Gao, S., Goh, B. L., et al.(2019). *Recent advances in non-toxic quantum dots and their biomedical applications,* Progress in Natural Science: Materials International, 29(6), s. 628-640. doi: 10.1016/j.pnsc.2019.11.007

[4] Vasudevan, D., Gaddam, R.R., Trinchi, A., Cole, I.(2015). *Core-Shell Quantum Dots: Properties and Applications*, Journal of Alloys and Compounds, 636, s. 395-404. doi: 10.1016/j.jallcom.2015.02.102

[5] Reshma, V.G., Mohanan, P.V.(2019). *Quantum dots: Applications and safety consequences,* Journal of Luminescence, 205, s. 287-298. doi: 10.1016/j.jlumin.2018.09.015.

[6] Zhu, S., Song, Y., Wang, J., Wan, H., Zhang, Y., Ning, Y., Yang, B., 2017. Photoluminescence mechanism in graphene quantum dots: Quantum confinement effect and surface/edge state. Nano Today 13, 10–14. https://doi.org/10.1016/j.nantod.2016.12.006

[7] Ray, S., Saha, A., Jana N. R., and Sarkar, R., Fluorescent Carbon Nanoparticles: Synthesis, Characterization, and Bioimaging Application. J. Phys. Chem. C, 2009, 113, 18546-18551. https://doi.org/10.1021/jp905912n

[8] Peng H., and Travas-Sejdic, J., Simple Aqueous Solution Route to Luminescent Carbogenic Dots from Carbohydrates, *Chemistry of Materials*, *21* (23), 5563-5565, 2009. DOI: 10.1021/cm901593y.

[9] Zhou, J., Booker, C., Li, R., Zhou, X., Sham, T.-K., Sun, X., and Ding, Z., An Electrochemical Avenue to Blue Luminescent Nanocrystals from Multiwalled Carbon Nanotubes (MWCNTs). Am. Chem. Soc., 129(4), 744-745, 2007. https://doi.org/10.1021/ja0669070.

[10] Shinde D.B., and Pillai, V.K., Electrochemical Preparation of Luminescent Graphene Quantum Dots from Multiwalled Carbon Nanotubes. Chem.–Eur. J., 18, 12522, 2012. https://doi.org/10.1002/chem.201201043.

[11] Zhu, H., Wang, X., Li, Y., Wang, Z., Yang F., and Yang, X., Microwave synthesis of fluorescent carbon nanoparticles with electrochemiluminescence properties. Chem. Commun., 5118-5120, 2009. DOI: 10.1039/B907612C

[12] Zhai, X., Zhang, P., Liu, C., Bai, T., Li, W., Dai L., and Liu, W., Highly luminescent carbon nanodots by microwave-assisted pyrolysis. Chem. Commun., 48(64), 7955-7957, 2012. doi: 10.1039/c2cc33869f.

[13] Liu, Y., Xiao, N., Gong, N., Wang, H., Shi, X., Gu, W., & Ye, L., One-Step Microwave-Assisted Polyol Synthesis of Green Luminescent Carbon Dots as Optical Nanoprobes. Carbon, 68, 258. 68, 258-264, 2014. https://doi.org/10.1016/j.carbon.2013.10.086

[14] Yang, Z.-C., Wang, M., Yong, A.M., Wong, S.Y., Zhang, X.-H., Tan, H., Chang, A.Y., Li X., and Wang. J., Intrinsically fluorescent carbon dots with tunable emission derived from hydrothermal treatment of glucose in the presence of monopotassium phosphate. Chem. Commun., 47(42), 11615-11617, 2011. DOI: 10.1039/C1CC14860E.

[15] Y. Yang, J. Cui, M. Zheng, C. Hu, S. Tan, Y. Xiao, Q. Yang and Y. Liu, One-step synthesis of amino-functionalized fluorescent carbon nanoparticles by hydrothermal carbonization of chitosan. Chem. Commun., 48, 380-382, 2012. DOI: 10.1039/C1CC15678K.

[16] De, B., & Karak, N., A green and facile approach for the synthesis of water soluble fluorescent carbon dots from banana juice. RSC Adv., 3, 8286-8290, 2013. DOI: 10.1039/c3ra00088e.

[17] Wang, Y., Hu, A., Carbon quantum dots: synthesis, properties and applications, J. Mater. Chem. C 2 (34), 6921-6139, 2014.

[18] Veli, S., Pinar, A., Characterization and catalytic performance of modified SBA-16 in liquid phase reaction. Int J Chem React Eng 16(8):20170246, 2018. https://doi.org/10.1515/ijcre-2017-0246

[19] Kaya, Ş., Şimşek, V. & Şahin, S., Investigation of Graphene Oxide/Mesoporous Silica Supports for Enhanced Electrochemical Stability of Enzymatic Electrodes. *Catal Lett* 154, 2701–2712, 2024. https://doi.org/10.1007/s10562-023-04520-x.

[20] Şimşek, V., & Mürtezaoğlu, K., Characterizations and catalytic activities investigation of synthesized solid-based heterogeneous catalysts in the esterification reaction. Anadolu Univ J Scie Technol A- Applied Scie and Eng., 19(2018), p.422-432, 2018. http://doi.org/10.18038/aubtda.357270

[21] Çubukçu, B., Meriçli., A.H., Mat, A., Sarıyar, G., Sütlüpınar, N ve Meriçli, F. İ.Ü., Eczacılık Fakültesi Farmakognozi Anabilim Dalı, Fitoterapi Yardımcı Ders Kitabı, 2002.

[22] Gündoğdu, M., Muradoğlu, F., Sensoy, R.I.G., Yılmaz, H., Determination of fruit chemical properties of Morus nigra L., Morus alba L. and Morus rubra L. by HPLC. Sci Hortic, 132: 37–41,2011.

[23] Suh, H.J., Noh, D.O., Kang, C.S., Kim, J.M., Lee, S.W., Thermal kinetics of color degradation of mulberry fruit extract. Nahrung/Food, 47(2): 132– 135, 2003.

[24] Mahesh, D.S., Vidhathri, B.S., Vidyashree, D.N., Narayanaswamy, T.K., Subbarayappa, C.T., Muthuraju, R., Biochemical Composition and Pharmacological Properties of Mulberry (Morus spp.) - A Review. Int J Curr Microbiol Appl Sci, 6(7): 2207–2217, 2017.

[25] Chen, P.N., Chu, S.C., Chiou, H.L., Kuo, W.H., Chiang, C.L., Hsieh, Y.S., Mulberry anthocyanins, cyanidin 3-rutinoside and cyanidin 3-glucoside, exhibited an inhibitory effect on the migration and invasion of a human lung cancer cell line. Cancer Lett, 235: 248–259, 2006.

[26] Souza da Costa, R., Ferreira da Cunha, W., Pereira, N., S., and Ceschin, A.M., An Alternative Route to Obtain Carbon Quantum Dots from Photoluminescent Materials in Peat. Materials , *11*(9), 1492, 2018. https://doi.org/10.3390/ma11091492.

[27] Kurdekar, A., Chunduri, L.A., Bulagonda, E.P. *et al.* Comparative performance evaluation of carbon dot-based paper immunoassay on Whatman filter paper and nitrocellulose paper in the detection of HIV infection. Microfluid Nanofluid 20, 99, 2016. https://doi.org/10.1007/s10404-016-1763-9

[28] Hsiao Wei, T., Rhelogy And Stability of Olive Oil Cream Emulsion Stabilized by Sucrose Fatty Acid Esters Nanionic Surfactans, Master Thesis, Malaya Kuala Lumpur University, Malezya, 2009.

[29] Kıyak Yıldırım, A., Şimşek, V., Investigation of the Effects Different H2SO4, HCI, HNO3 and HCIO4 Liguid Acid Media on the Synthesis of CdTe Semiconductor Thin Films for Solar Cells. JOTCSA. 11(2), 591-600,2024. https://doi.org/10.18596/jotcsa.1285341.

[30] Lu, W., Qin, X., Liu, S., Chang, G., Zhang, Y., Luo, Y., Asiri, A. M., Al-Youbi, A. O., Sun, X., Economical, Green Synthesis of Fluorescent Carbon Nanoparticles and Their Use as Probes for Sensitive and Selective Detection of Mercury(II) Ions, Anal. Chem., 84 (12), 5351- 5357,2012.